[19] Since the mixing ratio of the anions in the solution from which the crystals were grown was revealed to be almost identical to the stoichiometry determined by EPMA of the obtained crystal, the mixing ratio of the anions in the solution was adopted in the chemical formula of the crystal. The results of EPMA of λ-(BETS)$_2$Fe$_x$Ga$_{1-x}$Br$_{1.0}$Cl$_{3.0}$ are:
for $x = 0.50$, Fe/Ga/Br/Cl = 0.51:0.49:1.13:2.85 (0.50:0.50:1.00:3.00);
for $x = 0.40$, Fe/Ga/Br/Cl = 0.40:0.60:0.96:2.87 (0.40:0.60:1.00:3.00);
for $x = 0.30$, Fe/Ga/Br/Cl = 0.32:0.68:1.11:3.07 (0.30:0.70:1.00:3.00);
for $x = 0.20$, Fe/Ga/Br/Cl = 0.24:0.76:1.11:3.16 (0.20:0.80:1.00:3.00);
for $x = 0.10$, Fe/Ga/Br/Cl = 0.12:0.88:1.04:3.22 (0.10:0.90:1.00:3.00).

[20] Recent susceptibility measurements revealed that the angle between the easy axis of the antiferromagnetic structure and the c axis is about 35° in λ-(BETS)$_2$FeCl$_4$ (E. Ojima, T. Sasaki, private communication). While the easy axis of λ-(BETS)$_2$FeBr$_{0.6}$Cl$_{3.4}$ is approximately parallel to the b^* axis.

[21] M. Tokumoto, T. Naito, H. Kobayashi, A. Kobayashi, V. N. Laukhin, L. Brossard, P. Cassoux, *Synth. Met.* **1997**, *86*, 2161.

[22] L. Brossard, R. Clerac, C. Coulon, M. Tokumoto, T. Ziman, D. K. Petrov, V. N. Laukin, M. J. Naughton, A. Audouard, F. Goze, A. Kobayashi, H. Kobayashi, P. Cassoux, *Eur. Phys. J.* **1998**, *B1*, 439.

[23] H_C was reported to be about 20 kOe in [12]. Our recent measurements on single crystal λ-(BETS)$_2$FeBr$_{0.6}$Cl$_{3.4}$ with a rotating crystal in the a^*b^* plane gave more precious critical field.

Efficient Titanium Oxide/Conjugated Polymer Photovoltaics for Solar Energy Conversion**

By *Alexi C. Arango*, *Larry R. Johnson*, *Valery N. Bliznyuk*, *Zack Schlesinger*, *Sue A. Carter,** and *Hans-H. Hörhold*

Conjugated-polymer photovoltaics offer a non-toxic, easily manufactured, low-cost alternative to inorganic-based solar cells. The high absorption coefficient of most conjugated polymers and the high percentage of absorbed photons that produce an excited state (>90 %)[1] suggest that efficient photon to electron sensitivity is possible. Indeed, polymer photovoltaics demonstrating quantum efficiencies of almost 29 % at optimum wavelength have been fabricated through the use of interpenetrating donor–acceptor heterojunctions.[2] Such heterojunction photovoltaics are engineered to overcome the intrinsic limitations to photocurrent generation in conjugated polymers, which are short exciton diffusion lengths (often in the range of 10 nm), relatively large exciton binding energies (typically ~0.5 eV), and low electron mobilities (~10^{-9} cm^2/V s).[3,4]

Despite high quantum efficiencies, however, fill factors in donor–acceptor heterojunction photovoltaics remain low because resistive losses caused by poor hole transport in the active polymer have not yet been addressed. Zero-field hole mobilities in

[*] Prof. S. A. Carter, A. C. Arango, L. R. Johnson, Dr. V. N. Bliznyuk, Dr. Z. Schlesinger
Physics Department, University of California, Santa Cruz
Santa Cruz, CA 95064 (USA)
E-mail: sacarter@cats.ucsc.edu
Prof. H.-H. Hörhold
Institute of Organic and Macromolecular Chemistry
Friedrich Schiller University
D-07743 Jena (Germany)

poly(2-mehothoxy-5(2-ethyl)-hexoxy-*p*-phenylenevinylene (MEH–PPV), for example, are on the order of 10^{-7} cm^2/V s.[3] In this report, we describe an efficient inorganic/organic composite photovoltaic device containing a transparent planar titanium oxide (TiO$_x$) layer and a phenylamino-*p*-phenylenevinylene derivative (PA–PPV) which contains electron–donor moieties incorporated into the polymer backbone to enhance hole mobility[5] (Fig. 1). Efficient photogeneration of charge[6] and hole mobilities on the order of 10^{-4} cm^2/V s have been
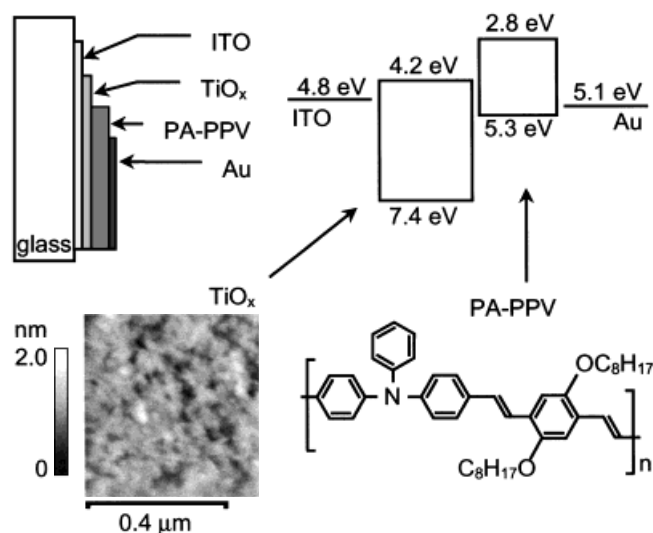

Fig. 1. The ITO/TiO$_x$/PA–PPV/Au device structure, energy-band diagram, and molecular structure of PA–PPV. An AFM image of the TiO$_x$ surface reveals surface-feature heights of less than 3 nm.

reported for PA–PVV.[7] The TiO$_x$ layer is distinguishable because it is employed as both an electron-accepting species and an anode. Moreover, it is smooth, transparent, and is easily spin-deposited via a sol-gel deposition route, in contrast to the porous layers used in dye-senstized solar cells.

Although the heterojunction interfacial area is low, we find that the external quantum efficiency (number of electrons collected/number of photons incident) of the device reaches 25 % at the absorption peak of the polymer. Additionally, by decreasing the thickness of the PA–PPV layer, we observe an increase in the fill factor, resulting in an increase in the power conversion efficiency. For an 80 nm PA–PPV film under white light illumination of 100 mW/cm^2, we achieve an open-circuit voltage of 0.85 V and a fill factor of 0.52, corresponding to a power efficiency of 3.9 % at 435 nm. We attribute the high monochromatic power efficiency to exciton diffusion to the TiO$_x$/PA–PPV interface, efficient dissociation at the interface and an enhanced hole mobility in PA–PPV. Our results suggest that the hole mobility of the active polymer material is the primary limit to even higher energy conversion efficiencies.

The *I–V* characteristics of our TiO$_x$ layered device (ITO/TiO$_x$/PA–PPV/Au) (ITO = indium tin oxide) and a more conventional device structure consisting of ITO and aluminum electrodes (ITO/PEDOT/PA–PPV/Al) (PEDOT = polyethylenedioctylthiophene) are presented in Figure 2. The dark cur-
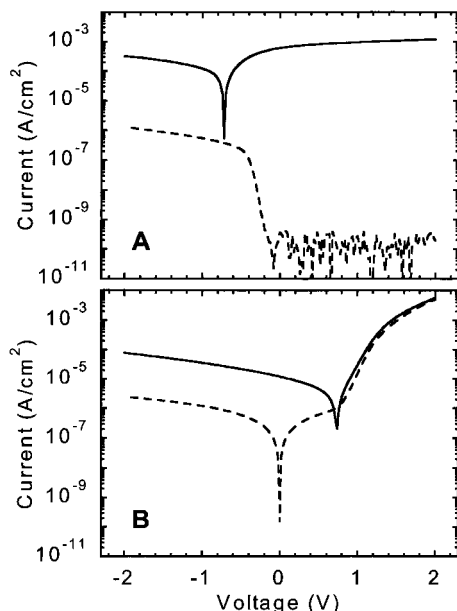
Fig. 2. Semi-logarithmic plots of the *I–V* characteristics in the dark (dashed line) and under white light illumination of approximately 100 mW/cm^2 (solid line) for A) an ITO/TiO$_x$/PA–PPV/Au device and B) an ITO/PEDOT/PA–PPV/Al device. The ITO is biased as the anode, which results in positive short-circuit current and negative open-circuit voltage for the TiO$_x$ device, and negative short-circuit current and positive open-circuit voltage for the Al device.

Fig. 3. The number of collected electrons per incident photon, or QE, versus the energy of an incident photon for an A) ITO/TiO$_x$/PA–PPV(80 nm)/Au device and an B) ITO/PEDOT/PA–PPV(100 nm)/Al. The absorption coefficient (α) of PA–PPV is plotted on the *y*-axis to the right. Illumination is through the TiO$_x$ in A) and the Al in B).

rent in forward bias in the TiO$_x$ layered device is suppressed due to blocking of hole injection from the ITO electrode. Under illumination in forward bias, the photocurrent saturates and the zero bias photocurrent is enhanced by almost two orders of magnitude over that of the Al device. In the TiO$_x$ layered device, the absence of current in the dark and the enhancement of current in the light imply photo-induced charge transfer from PA–PPV to the TiO$_x$ layer, as previously identified.[8] The open-circuit photovoltage of the TiO$_x$ layered device is –0.7 V, while the photovoltage produced by the Al device is +0.7 V, indicating the ability of the TiO$_x$ conduction band to determine the internal field and thereby function as anode analogous to the metal/insulator/metal model.[9]

The photocurrent action spectra with zero applied bias of both the TiO$_x$ layered device and the Al device are presented in Figure 3. In both cases, the diodes are illuminated through the electron-accepting electrode and the quantum efficiency (QE) includes a correction for reflective losses. For the TiO$_x$ layered device, the QE approaches its maximum value near the absorption maximum of the polymer at approximately 2.8 eV, while the Al device efficiency remains flat over the absorption region of the polymer. The QE at 2.8 eV of the TiO$_x$ layered device is over 50 times greater than the QE of the Al device. Such an enhancement implies that a mechanism other than simply the positioning of the electron energy levels throughout the device is responsible for the efficient generation and separation of charge.

By modifying the PA–PPV film thickness and analyzing the fill factor, we gain insight into the charge generation process in the TiO$_x$ layered cell (Fig. 4). The fill factor (FF) is defined as the maximum power that can be delivered to an external
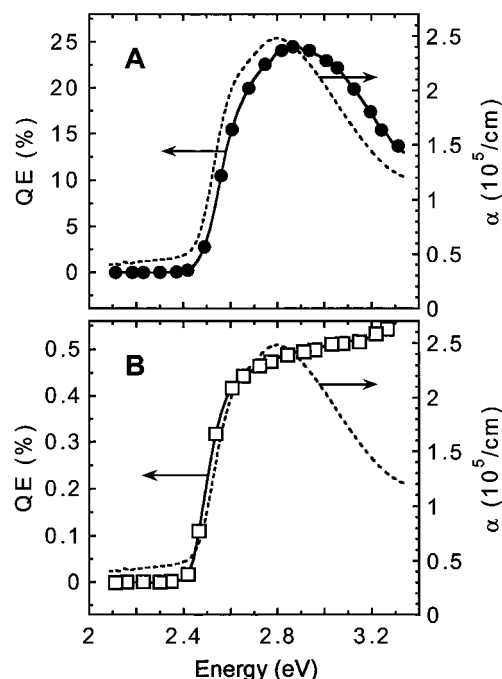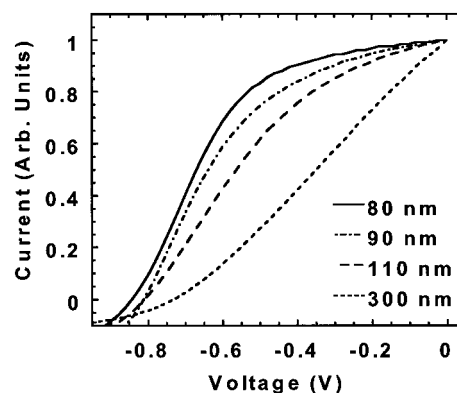

Fig. 4. The normalized photogenerated current versus the voltage applied in the direction opposing current flow for TiO$_x$ layered devices with a PA–PPV film thickness of 80 nm (—), 90 nm (· –), 110 nm (– –), and 300 nm (- - -). The white-light illumination intensity is approximately 100 mW/cm^2 from a xenon lamp. The fill factor increases with decreasing PA–PPV film thickness.

load divided by the product of the short-circuit current and the open-circuit voltage. At solar illumination intensities of 100 mW/cm^2, a sample with a PA–PPV layer of 300 nm yields a FF of 0.24; a 110 nm film yields a FF of 0.37; a 90 nm film yields a FF of 0.45; and an 80 nm film yields a FF of 0.52. At low illumination intensities, the fill factor of all TiO$_x$ layered devices reaches or exceeds 0.60, while pure devices display fill factors in the range of 0.25 regardless of illumination intensity (data not shown).

The shape and magnitude of the photocurrent action spectrum for the TiO$_x$ layered device confirm that photo-excitons

which result in photocurrent originate at the TiO$_x$/PA–PPV heterojunction, that the exciton diffusion length to this interface is long,[10] and that exciton dissociation efficiency at the interface is high.[11] The symbatic form of the photocurrent action spectrum implies that the active interface is the illuminated interface—the TiO$_x$/PA–PPV heterojunction.[12] The magnitude of a symbatic photocurrent action spectrum is determined by two fundamental factors: the distance that an exciton can travel to reach the dissociation interface and the percent of excitons at the interface that dissociate without recombining. Since the percentage of photons absorbed within the exciton diffusion length must be greater than the magnitude of the quantum efficiency, we are forced to consider diffusion lengths in PA–PPV greater than those typically reported for PPV. In PPV, the exciton diffusion length is 9 ± 1 nm,[4] yet only 15 % of incident photons are absorbed in a PA–PPV film of 10 nm, assuming an exponential extinction of light. If we presume, for example, that 80 % of excitons generated within the diffusion length of the TiO$_x$ interface contribute to a quantum efficiency of 25 %, then a diffusion length of 20 nm is required.

The relatively low quantum efficiency observed in the Al electrode device suggests that the interfacial dissociation efficiency is not simply determined by the difference between donor and acceptor energy levels, but is highly dependent on the metallic or semiconducting properties and/or the physical/chemical interfacial arrangement. Obstruction of injection at a metal on polymer interface is likely due to interference effects,[13] an image force potential,[14] interface chemistry or an interfacial oxide layer.[15] In contrast, adsorption of the polymer onto the TiO$_x$ surface due to non-bonding electrons associated with oxygen and nitrogen groups in PA–PPV will result in a spatially intimate contact between the polymer's conjugated chain and the TiO$_x$ surface, which will allow orbital overlap at the interface and thereby promote charge transfer.

The observation of high fill factors in TiO$_x$/thin PA–PPV devices at high illumination intensities is consistent with exciton diffusion and dissociation. Increasing the applied bias from zero bias to 0.3–0.4 V in the direction opposing the flow of photocurrent results in only a small decrease in the photocurrent. Such bias independence implies that, at low voltages, charge generation is predominantly a field-independent process. Exciton generation and dissociation in the bulk is expected to be strongly field dependent,[16] yet the diffusion of an exciton (a neutral excited state) is not. Following dissociation, the remaining electron in the TiO$_x$ diffuses away from the interface,[17] while the remaining hole is removed by the internal field and/or diffusion (Fig. 5). Subsequently, transport of both charge carriers contributes to the internal resistive losses that degrade the power efficiency of the cell.

The removal of excited electrons and holes from a photovoltaic device should be balanced in order to prevent uneven charge build up that would result in an electric field opposing the built-in internal field. The electron mobility through a nanoporous TiO$_2$ film is 1 cm^2/V s.[18] However, PA–PPV hole mobilities are four orders of magnitude lower.[7] Resistive
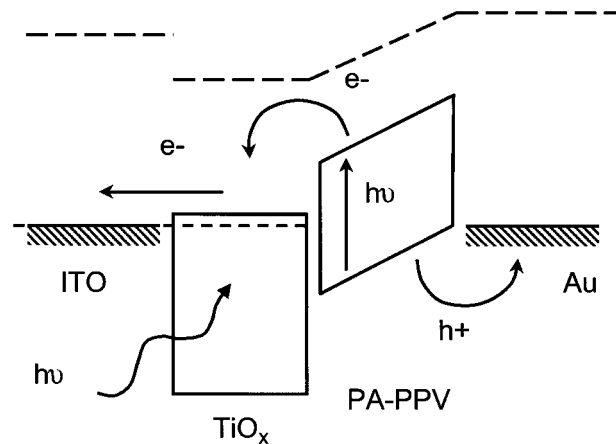

Fig. 5. The electron energy-level schematic of device operation under illumination in short-circuit conditions. An incident photon in the visible passes through the TiO$_x$ layer and is absorbed by the polymer (PA–PPV) whereby an exciton is produced and may diffuse a distance of up to 20 nm towards the TiO$_x$/polymer interface. Interfacial exciton dissociation occurs via electron transfer to the TiO$_x$, resulting in population of the TiO$_x$ conduction band, elevation of the TiO$_x$ Fermi level and formation of a Schottky barrier at the TiO$_x$/ITO interface (not shown). Electron diffusion through the TiO$_x$ layer, injection into the ITO, and redistribution of charge through the external circuit, such that the TiO$_x$, ITO, and Au Fermi levels are aligned, produces an internal field across the polymer layer. Hole transport through the polymer layer under the influence of this internal field is required to complete the circuit and is believed to be the main source of resistive losses in the cell.

losses in PA–PPV will, therefore, limit the fill factor and thus the power conversion efficiency at solar intensities. Since the power dissipated due to resistive losses increases as the square of the current flowing through a resistive layer, this effect is less important at low intensities, yet becomes significant at one-sun solar intensities (100 mW/cm^2).

The layered TiO$_x$/PA–PPV device configuration described here represents a robust and adaptable preliminary device design from which considerable improvements in organic-based solar cell efficiency, cost and stability can be realized. Since it is the difference between the position of the conduction band-edge of the TiO$_x$ and the work function of the back contact which determines the open-circuit voltage, stable low-cost materials with high workfunctions, such as carbon or silver paint, can be used as the back electrode. With the addition of a third material, a hole-transport species, we expect that the obstacle of low polymer hole mobilities can be overcome. This would allow the fabrication of devices with increased interfacial active area and thickness.[19] Given that the TiO$_x$ layered cells are transparent to light below the polymer absorption edge, we envision stacking individual cells in series to obtain high efficiency multilayered structures that capture the power of the full solar or to use smaller bandgap polymers. Finally, we note that while the device structure presented here is similar to a solid-state dye-sensitized cell,[20] the ability of the polymer to serve as both the charge generating and transporting species allows one to obtain faster device operation and high effiencies without requiring the diffusion of a polymer into the confined geometry of a porous network.

In conclusion, we have demonstrated a polymer-based photovoltaic cell structure suitable for low-cost solar energy conver-

sion owing to a high quantum efficiency, high open-circuit voltage, and high fill factor at one-sun illumination intensities. Further development of polymer-based heterojunction photovoltaics will require the enhancement of hole transport through the cells and absorption throughout the visible spectrum.

Experimental

A complete and dense TiO$_x$ film is prepared using the TiO$_2$ precursor titanium ethoxide, Ti(OCH$_2$CH$_3$)$_4$ (Gelest, Inc.). By volume, 4 parts of Ti ethoxide is added to a solution of 40 parts ethyl alcohol, which contains 1 part water and has a pH of 1 adjusted with the addition of hydrochloric acid (Aldrich). The TiO$_2$ precursor is spin-coated onto ITO patterned glass at 1000 rpm to complete the sol–gel synthesis. The resulting TiO$_x$ film thickness ranges from 100 to 50 nm, as measured by atomic force microscopy (AFM). The sample is heated under vacuum at 78 °C for 45 min to allow further cross-linking (condensation) and dehydration of the TiO$_x$ matrix. The resulting film is amorphous [21]. Annealing at 450 °C for 30 min (densification) allows the growth of crystalline regions of the anatase phase. The TiO$_x$ film is transparent and smooth, with surface features less than 3 nm.

The TiO$_x$ film is transferred into a dry box under nitrogen atmosphere where conjugated polymer poly(N-phenylimino-1,4-phenylene-1,2-ethenylene-1,4-(2,5-dioctoxy)-phenylene-1,2-ethenylene-1,4-phenylene), PA–PPV, (3 % by weight solution in p-xylene) is spin-coated at 1000–4000 rpm, which produces films of 120–80 nm, respectively. The sample is then placed either on a hot plate at 80 °C or in a vacuum chamber overnight to remove solvent residue. A 35 nm layer of gold (Au) is thermally evaporated on top of the polymer, leaving an active area of 3 mm^2.

For comparison, we fabricate an ordinary polymer diode with a semi-transparent aluminum (Al) top contact. A thin layer of PEDOT, which has a work function of 5.0 eV is spin deposited on top of the ITO coated glass. Since the work function of Al (4.2 eV) is near the TiO$_x$ conduction band, the Al is intended to replace the TiO$_x$ as the electron accepting anode, while the PEDOT is intended to replace the Au cathode. All measurements are performed in a nitrogen atmosphere.

- [1] M. Yan, L. J. Rothberg, F. Papadimitrakopoulos, M. E. Galvin, T. M. Miller, *Phys. Rev. Lett.* **1994**, *72*, 1104.
- [2] G. Yu, J. Gao, J. C. Hummelen, F. Wudl, A. J. Heeger, *Science* **1995**, *270*, 1789. M. Granström, K. Petritsch, A. C. Arias, A. Lux, M. R. Anderson, R. H. Friend, *Nature* **1998**, *395*, 257.
- [3] L. Bozano, S. A. Carter, J. C. Scott, G. G. Malliaras, P. J. Brock, *Appl. Phys. Lett.* **1999**, *74*, 1132.
- [4] R. H. Friend, G. J. Denton, J. J. M. Halls, N. T. Harrison, *Solid State Commun.* **1997**, *102*, 249.
- [5] H. Rost, A. Teuschel, S. Pfeiffer, H.-H. Hörhold, *Synth. Met.* **1997**, *84*, 269. S. Pfeiffer, H. Rost, H.-H. Hörhold, *Macromol. Chem. Phys.* **1999**, *200*, 2411.
- [6] T. K. Däubler, H. Rost, H.-H. Hörhold, D. Neher, *Phys. Rev. B* **1999**, *59*, 1964. T. K. Däubler, S. Pfeipher, H.-H. Hörhold, D. Neher, *Opt. Mater.* **1999**, *12*, 373.
- [7] D. Hertel, H. Bässler, U. Scherf, H.-H. Hörhold, *J. Chem. Phys.* **1999**, *110*, 9214.
- [8] A. C. Arango, P. J. Brock, S. A. Carter, *Appl. Phys. Lett.* **1999**, *74*, 1698.
- [9] G. G. Malliaras, J. R. Salem, P. J. Brock, J. C. Scott, *J. Appl. Phys.* **1998**, *84*, 1583.
- [10] T. J. Savenije, J. M. Warman, A. Goossens, *Chem. Phys. Lett.* **1998**, *287*, 148.
- [11] P. A. van Hal, M. P. T. Christiaans, M. M. Wienk, J. M. Kroon, R. A. J. Janssen, *J. Phys. Chem. B* **1999**, *103*, 4352.
- [12] M. G. Harrison, J. Grüner, G. C. W. Spencer, *Phys. Rev. B* **1997**, *55*, 7831.
- [13] H. Becker, S. E. Burns, R. H. Friend, *Phys. Rev. B* **1997**, *56*, 1893.
- [14] M. M. Bussac, D. Michoud, L. Zuppiroli, *Phys. Rev. Lett.* **1998**, *81*, 1678.
- [15] R. H. Friend, R. W. Gymer, A. B. Holmes, J. H. Burroughes, *Nature* **1999**, *397*, 121.
- [16] V. I. Arkhipov, E. V. Emelianova, H. Bässler, *Phys. Rev. Lett.* **1999**, *82*, 1321.
- [17] A. Solbrand, H. Lindstrom, H. Rensmo, A. Hagfeldt, S. Lindquist, *J. Phys. Chem. B* **1997**, *101*, 2514.
- [18] *Semiconductor Electrodes* (Ed: H. O. Finklea), Elsevier, Amsterdam **1988**.
- [19] The thickness that is required for the active polymer to absorb a large fraction of the incident light is $1/\alpha$. In the case of PA–PPV, this thickness is 100–200 nm.
- [20] U. Bach, D. Lupo, P. Comte, J. E. Moser, M. Grätzel, *Nature* **1998**, *395*, 593.
- [21] M. Zaharescu, M. Crisan, I. Mosevic, *J. Sol–Gel Sci. Technol.* **1998**, *13*, 769.

Encapsulation of Poly(*N*-Isopropyl Acrylamide) in Silica: A Stimuli-Responsive Porous Hybrid Material That Incorporates Molecular Nano-Valves**

By *G. V. Rama Rao* and *Gabriel P. López**

This paper describes the synthesis of hybrid materials composed of poly(N-isopropylacrylamide) (PNIPAAM) encapsulated in silica for use as switchable membranes in which permeability can be controlled by the solubility behavior of PNIPAAM. The encapsulated PNIPAAM molecules can act as "nano-valves" whose molecular permeability can be controlled by cycling through the aqueous lower critical solution temperature (LCST) of the PNIPAAM component. PNIPAAM-silica membranes were supported on porous centrifugal filters (Millipore YM-30) by coating with precursors prepared by the sol-gel process. Permeation experiments on PNIPAAM–silica membranes with solutions of various molecular weights of poly(ethylene glycol) (PEG) have clearly demonstrated that the membranes thus formed function as switchable molecular filters. Under controlled pressure, these membranes are impermeable to water below the LCST. At the same pressures, when the temperature is raised above the LCST (~31 °C) the membranes become permeable to aqueous solutions of PEGs of low molecular weight (≤5000 Da) while being impermeable to PEGs of higher molecular weight. These results suggest that it should be possible to create tunable molecular filters that incorporate such nano-valves from hybrid materials prepared by simple synthetic methods.

PNIPAAM belongs to an important class of thermo-responsive smart (or stimuli-responsive) polymers that exhibit interesting solubility behavior in aqueous media.[1,2] It shows inverse solubility upon heating and undergoes a critical transition from a hydrophilic (extended chain conformation) to hydrophobic (compacted conformation) at a temperature known as LCST. The reduction in excluded volume associated with this transition has been reported to be more than a factor of 300 for PNIPAAM in solution.[3] This property has been exploited in several applications in biotechnological areas.[2,4–9] For example, hydrogels of PNIPAAM have been used in concentration and separation of proteins.[8,9] Smart polymers such

[*] Prof. G. P. Lopez, Dr. G. V. Rama Rao
Center for Micro-Engineered Materials
Department of Chemical and Nuclear Engineering
209 Farris Engineering Center, The University of New Mexico
Albuquerque, NM 87131-1341 (USA)
E-mail: gplopez@unm.edu